AGU PUBLICATIONS

JGR

Journal of Geophysical Research: Atmospheres

RESEARCH ARTICLE
10.1002/2015JD023137

Key Points:
- We investigate air temperature spatial distribution over three mountain glaciers
- Observations can be explained by katabatic winds and external warming
- We propose a simple model to explain the observed spatial distribution patterns

Correspondence to:
A. Ayala,
ayala@ifu.baug.ethz.ch

Citation:
Ayala, A., F. Pellicciotti, and J. M. Shea (2015), Modeling 2 m air temperatures over mountain glaciers: Exploring the influence of katabatic cooling and external warming, *J. Geophys. Res. Atmos.*, *120*, 3139–3157, doi:10.1002/2015JD023137.

Received 20 JAN 2015
Accepted 16 MAR 2015
Accepted article online 19 MAR 2015
Published online 18 APR 2015

Modeling 2 m air temperatures over mountain glaciers: Exploring the influence of katabatic cooling and external warming

A. Ayala[1], F. Pellicciotti[1,2], and J. M. Shea[3]

[1]Institute of Environmental Engineering, ETH Zurich, Zurich, Switzerland, [2]Department of Geography, Faculty of Engineering and Environment, Northumbria University, Newcastle, UK, [3]International Centre for Integrated Mountain Development, Kathmandu, Nepal

Abstract Air temperature is one of the most relevant input variables for snow and ice melt calculations. However, local meteorological conditions, complex topography, and logistical concerns in glacierized regions make the measuring and modeling of air temperature a difficult task. In this study, we investigate the spatial distribution of 2 m air temperature over mountain glaciers and propose a modification to an existing model to improve its representation. Spatially distributed meteorological data from Haut Glacier d'Arolla (Switzerland), Place (Canada), and Juncal Norte (Chile) Glaciers are used to examine approximate flow line temperatures during their respective ablation seasons. During warm conditions (off-glacier temperatures well above 0°C), observed air temperatures in the upper reaches of Place Glacier and Haut Glacier d'Arolla decrease down glacier along the approximate flow line. At Juncal Norte and Haut Glacier d'Arolla, an increase in air temperature is observed over the glacier tongue. While the temperature behavior over the upper part can be explained by the cooling effect of the glacier surface, the temperature increase over the glacier tongue may be caused by several processes induced by the surrounding warm atmosphere. In order to capture the latter effect, we add an additional term to the Greuell and Böhm (GB) thermodynamic glacier wind model. For high off-glacier temperatures, the modified GB model reduces root-mean-square error up to 32% and provides a new approach for distributing air temperature over mountain glaciers as a function of off-glacier temperatures and approximate glacier flow lines.

1. Introduction

Air temperature is a key variable within the energy balance equations for snow and ice surfaces, and because it is frequently correlated with other meteorological variables, it is also used as an index variable in empirical melt models [*Ohmura*, 2001; *Hock*, 2003, 2005]. Due to the complex micrometeorology of mountainous environments and the typical lack of detailed measurements on glaciers, linear lapse rates are commonly used to estimate spatially distributed air temperature fields for glacier melt estimations [*Hock*, 1999; *Klok and Oerlemans*, 2002; *Hock and Holmgren*, 2005; *Michlmayr et al.*, 2008; *Shea et al.*, 2009; *Ragettli and Pellicciotti*, 2012; *Pellicciotti et al.*, 2014]. Melt calculations are highly sensitive to the specified lapse rates, especially when lapse rates derived from low- or medium-elevation sites are extrapolated to high-elevation sites [e.g., *Ragettli and Pellicciotti*, 2012; *Pellicciotti et al.*, 2014]. While mean daily or seasonal lapse rates are often used to estimate near-surface air temperatures, hourly lapse rates contain additional climatic information that leads to significantly improved temperature estimates [*Gardner and Sharp*, 2009; *Gardner et al.*, 2009; *Petersen and Pellicciotti*, 2011; *Pellicciotti et al.*, 2014]. In this article, we define a lapse rate as the change in air temperature with increasing elevation and we specify if the lapse rate is negative (e.g., typical decrease with elevation) or positive.

Katabatic winds are a characteristic local meteorological feature on temperate alpine glaciers that affect both the near-surface air temperature distribution and the turbulent fluxes [*Hoinkes*, 1954; *van den Broeke*, 1997a; *Denby and Greuell*, 2000; *Oerlemans and Grisogono*, 2002]. Katabatic winds form in environments where the air layer in contact with the glacier surface is cooler than surrounding air masses, and well-developed katabatic winds are common when the glacier surface reaches the melting point. In such situations, the glacier surface temperature has a maximum of 0°C, excess energy at the surface is directed to melt, and a constant boundary condition is provided for the atmospheric system. The cooler, denser air consequently flows down the glacier along the flow line and modifies the near-surface air temperature distribution [*Oerlemans*, 1998; *Munro*, 2006].

Numerous observations of katabatic winds have been reported over mountain glaciers and a number of factors affect their development. While fetch length, funneling effect, and temperature difference between the atmosphere and the glacier surface strengthen the katabatic wind layer [*van den Broeke*, 1997b; *Greuell and Böhm*, 1998; *Oerlemans and Grisogono*, 2002; *Munro*, 2006; *Pigeon and Jiskoot*, 2008], the influence of synoptic winds, entrainment of warm air from the upper layer, turbulent mixing with up-valley winds, and heat advection from mountain walls will weaken it [*van den Broeke*, 1997b; *Greuell and Böhm*, 1998; *Hannah et al*., 2000; *Oerlemans and Grisogono*, 2002; *Munro*, 2006; *Jiskoot and Mueller*, 2012]. Radiative cooling and the Coriolis force are also relevant in other types of environment, like large sloping ice sheets [e.g., *Gardner et al*., 2009; *Vihma et al*., 2011]. A critical air temperature threshold that denotes the onset of the katabatic boundary layer development was identified by *Shea and Moore* [2010] using a set of meteorological measurements on three glaciers in the southern Coast Mountains of British Columbia over three ablation seasons. They also found that stronger cooling effects at greater flow distances implies a lower climatic sensitivity to external temperature changes. A similar idea was used by *Jiskoot and Mueller* [2012] on the Shackleton Glacier, Canadian Rockies. They implemented a surface energy balance model in which katabatic winds were switched on and off depending on the air temperature measured in the proglacial valley.

In order to understand how air temperatures are distributed over a melting glacier during katabatic wind episodes, *Greuell and Böhm* [1998] proposed a simple thermodynamic glacier wind model (the GB model) that focused on air temperature variations along the glacier flow line. The GB model, which was developed and tested using data from the glaciometeorological experiment Pasterze Experiment (PASTEX) [*Greuell et al*., 1994], solves the energy balance of an air parcel traveling down along an infinite glacier slope with a temperature of 0°C. The model considers only two effects: the cooling of the down-flowing air through sensible heat exchange with the glacier surface and the simultaneous warming due to adiabatic compression. Using these two processes, the model provides a simple 2 m air temperature distribution as a function of the distance along the flow line and quantifies the sensitivity of the air in contact with the glacier surface to off-glacier temperature variations. Climatic sensitivity was defined as the ratio of changes in the air temperature 2 m above the glacier surface to changes in temperature outside the thermal regime of the glacier [*Greuell and Böhm*, 1998].

Few applications of the GB model are found in the literature. In the original paper, the model successfully reproduced the observed air temperature distribution over Pasterze Glacier [*Greuell and Böhm*, 1998]. Later, *Petersen et al*. [2013] tested the GB model on Haut Glacier d'Arolla (Switzerland) over one ablation season. In order to improve the model performance, they assumed, in contrast to the original model, that the katabatic layer thickness varies along the glacier flow line. In fact, because the GB model assumes an infinite glacier slope at a temperature of 0°C, air temperature asymptotically reaches an equilibrium with a characteristic length scale. This equilibrium value is theoretically reached at the same location where climatic sensitivity reaches a value of zero and temperatures are entirely controlled by katabatic winds. Nevertheless, air temperature observations over glacier tongues show an increase with distance along the flow line [*Pellicciotti et al*., 2008; *Petersen and Pellicciotti*, 2011; *Petersen et al*., 2013]. In a recent application of the GB model to three glaciers of the Italian Alps, *Carturan et al*. [2014] found good agreement between the GB model and their observations, except for weather stations close to the glacier terminus where the air temperatures were higher than expected. This behavior is not well explained by the GB model and suggests the presence of other physical processes that may disturb the katabatic layer, e.g., entrainment of warm air from the upper layer, enhanced terrain irradiance and turbulent mixing with up-valley winds.

In this study, we investigate and compare the spatial distribution of air temperature at three glaciers in Switzerland, Canada, and Chile. These different study sites span a wide range of geographic, climatic, and geomorphological characteristics. We aim to improve the distributed modeling of air temperature over mountain glaciers and provide an alternative to constant and uniform linear lapse rates. For this, we add a linear term to the GB equation that attempts to describe the effect of additional heating observed over glacier tongues.

The remainder of this paper is organized as follows: In sections 2 and 3, we describe the study sites and the collected data sets. In section 4, we describe the GB model and propose a modification based on the observations and conclusions of section 3. In section 5, we compare observed and estimated near-surface temperatures and evaluate the performance of the modified GB model, the original GB model and linear lapse rates. Finally, in sections 5 and 6, we present and discuss our main findings.

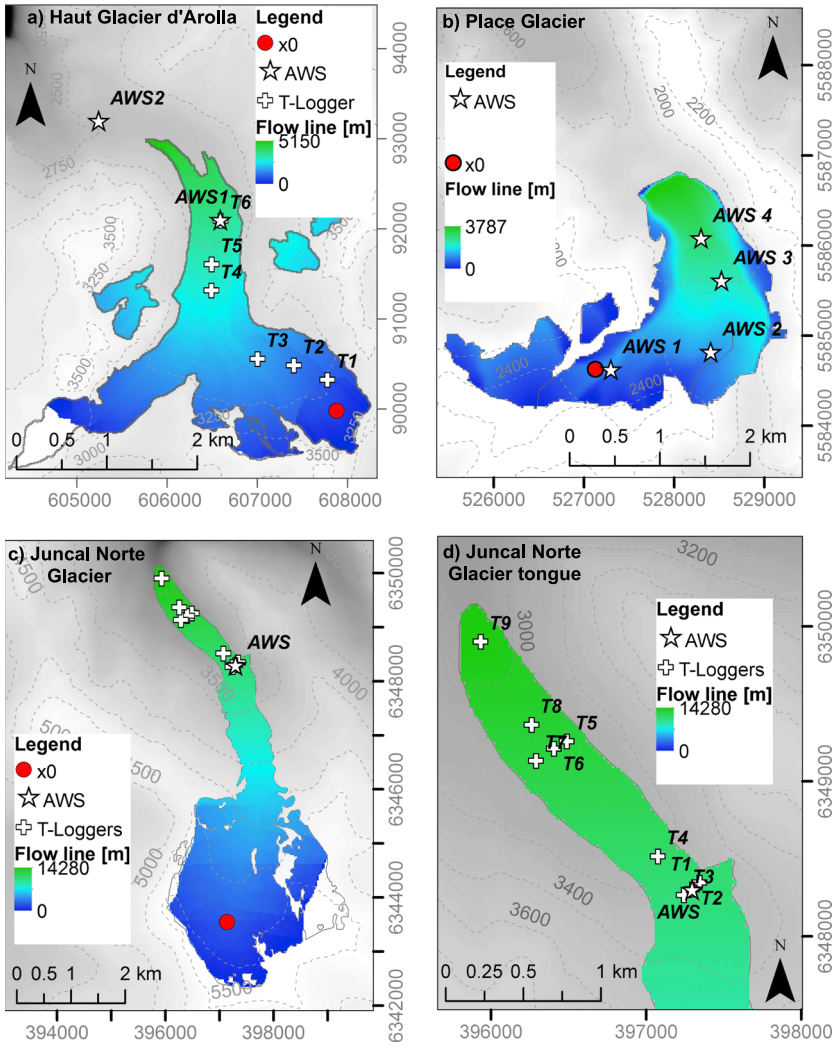

Figure 1. Map of Haut Glacier d'Arolla (Switzerland), Place (Canada), and Juncal Norte (Chile) Glaciers. Meteorological stations correspond to automatic weather stations (AWS) and temperature loggers (T-loggers). Glacier outlines are filled with the distributed flow lines. Coordinate systems are CH1903 for Switzerland and WGS84 for Canada and Chile. White surfaces on glacier borders hydraulically contribute to neighbor catchments. In Place Glacier the position selected for x_0 coincides with the AWS1.

2. Study Sites

We analyze spatially distributed data sets of air temperature collected during the ablation season over Haut Glacier d'Arolla, Place Glacier, and Juncal Norte Glacier, which are located in Switzerland, Canada, and Chile, respectively (Figure 1 and Table 1). Previous studies have reported the presence of katabatic winds at all three study sites [*Strasser et al.*, 2004; *Pellicciotti et al.*, 2008; *Shea and Moore*, 2010; *Petersen and Pellicciotti*, 2011; *Petersen et al.*, 2013].

Table 1. Glacier Locations and Main Characteristics

Glacier	Country	Location (Latitude, Longitude)	Area (km^2)	Elevation Range (m asl)	Flow Line Length (km)	Average Slope (°)
Haut Glacier d'Arolla	Switzerland	45.97°N 7.53°E	4.5	2550–3520	5.1	17.4
Place	Canada	50.42°N 122.62°W	3.5	1830–2560	3.8	13.8
Juncal Norte	Chile	33.02°S 70.10°W	7.6	2900–5910	14.3	26.7

Haut Glacier d'Arolla is a small ($<5\,km^2$) temperate glacier located in the Val d'Herens, in Valais, Switzerland on the main Alpine divide. The glacier has an upper area with a northwesterly aspect and a northward flowing glacier tongue. Extensive glaciological research has been conducted on this glacier describing its energy and mass balances, hydrology, geochemistry, and ice dynamics [e.g., *Arnold et al*., 1996; *Brock and Willis*, 2000; *Strasser et al*., 2004; *Pellicciotti et al*., 2005; *Dadic et al*., 2008; *Petersen et al*., 2013]. The upper area of Haut Glacier d'Arolla is relatively open. Down-glacier winds are weak in comparison to those of the lower tongue, and thus, synoptic winds often prevail. In contrast, the lower narrow valley leads to convergence acceleration of the wind flow, which shows higher average speed and directional consistency than in the upper area [*Strasser et al*., 2004]. During the last decades, negative mass balances and glacier retreat have favored the emergence and expansion of debris covered areas that might raise the near-surface air temperature relative to that above bare ice surfaces [*Reid et al*., 2012].

Place Glacier is located in the southern Coast Mountains of British Columbia, Canada. In this mountainous region, proximity to the Pacific Ocean produces strong gradients between maritime and continental climatic regimes, and winters are characterized by high snow accumulation. Place Glacier sits on the eastern edge of a glacierized area and is a small alpine glacier ($<4\,km^2$) with a more continental climatic setting and lower snow accumulation than areas to the west. A small accumulation area, sheltered from prevailing westerly flows, leads to a wide, low-angle ablation area. In contrast to Haut Glacier d'Arolla and Juncal Norte Glacier, whose elevations span 970 m and 3010 m, respectively, Place Glacier has an elevation range of only 730 m. According to *Munro and Marosz-Wantuch* [2009], the accumulation area is susceptible to topographic steering of entrained synoptic airflow and the glacier wind coming from the upper area may diverge to the northern and southern tongues. Mass balance investigations on Place Glacier started in 1965 in the context of the International Hydrological Decade [*Moore and Demuth*, 2001; *Shea et al*., 2004, 2009; *Shea and Moore*, 2010].

Juncal Norte Glacier is located in the semiarid Andes of central Chile. This is a region characterized by high altitudes (reaching 6000 m above sea level (asl)), mild wet winters and dry summers with almost zero precipitation, with the exception of easterly convective storms [*Garreaud et al*., 2009]. Juncal Norte Glacier has an area of $7.6\,km^2$ and flows northward along a narrow valley surrounded by steep slopes from about 6100 to 2900 m asl. Glaciological research conducted here during the past decade has focused on the characterization of its energy and mass balance and hydrological processes [*Corripio and Purves*, 2005; *Bown et al*., 2008; *Pellicciotti et al*., 2008; *Petersen and Pellicciotti*, 2011; *Ragettli and Pellicciotti*, 2012].

3. Data Analysis

3.1. Description of Available Data

The data set in this study consists of spatially distributed air temperature measurements recorded at temperature loggers (T-loggers) and meteorological variables registered at automatic weather stations (AWS) (Figure 1 and Table 2). At Haut Glacier d'Arolla and Place Glacier, measurements are distributed along the length of the glacier. However, due to the extremely difficult access to the upper sections of Juncal Norte Glacier, this glacier has measurements only over the glacier tongue. All data were recorded at time intervals of 5 to 10 min. We use hourly averaged data for all analyses.

T-loggers at Haut Glacier d'Arolla and Juncal Norte Glacier consisted of a temperature sensor (HOBO H8 Pro Temp) with integrated data logger housed in a shielded PVC cylinder and fixed to a metal tripod of 2 m height. The ventilation of the T-loggers is allowed by channelized wind flow in the PVC cylinders. The accuracy of these instruments ranges between 0.2 and 0.5°C on average. T-logger data are strongly correlated to reference AWS measurements, but an adjustment of -0.5°C was applied to correct a positive temperature bias that is likely caused by the more deficient ventilation system of the T-loggers in comparison to the AWSs [*Petersen and Pellicciotti*, 2011; *Petersen et al*., 2013]. On Place Glacier temperatures were measured at floating automatic weather stations equipped with Rotronic SC2 temperature and relative humidity sensors housed in standard unventilated radiation shields. Accuracy of air temperature and relative humidity sensors are 0.2°C and 1.5% (at 23°C), respectively [*Shea and Moore*, 2010].

We use digital elevation models (DEMs) derived from light detection and ranging (lidar) flights over Haut Glacier d'Arolla (10 m resolution) and Place Glacier (25 m resolution). On Juncal Norte Glacier we use a 30 m resolution DEM obtained from the Aster Global Digital Elevation Model (GDEM) project version 2

Table 2. Description of Collected Data During Field Studies

Glacier	Period of Measurement	Air Temperature Station	Elevation (m asl)	Distance Along the Flow Line (From x_0) (m)	Number of Hours With Complete Measurements
Haut Glacier d'Arolla	23:00 25 May 2010	1	2992	120	1284
		2	2946	669	
	22:00 22 Aug 2010	3	2891	1141	
		4	2897	2175	
		5	2886	2465	
		6	2792	2911	
Place	10:00 29 Jul 2007	1	2294	0	527
		2	2075	66	
	10:00 15 Sep 2007	3	1999	1198	
		4	1938	1859	
Juncal Norte	19:00 08 Dec 2008	1	3306	6634	897
		2	3305	6555	
	00:00 04 Feb 2009	3	3307	6527	
		4	3238	6870	
		5	3134	7932	
		6	3126	7865	
		7	3119	7735	
		8	3100	8062	
		9	3000	8809	

(http://gdem.ersdac.jspacesystems.or.jp) [*Aster GDEM Validation Team*, 2011; *Tachikawa et al*., 2011]. Finally, for each glacier, we choose a set of meteorological stations outside the glacier thermal influence and we consider them as representative of off-glacier conditions (Table 3).

3.2. Exploratory Analysis of Field Data

In order to understand how air temperature distribution over mountain glaciers varies under the influence of the surrounding atmosphere, we investigate the relation between on-glacier air temperature distribution and off-glacier temperatures. For this, we plot distributed measurements of air temperature, classified according to percentiles of off-glacier temperatures, as a function of the distance along the glacier flow line and elevation.

Glacier flow lines are calculated using the DEMs described above, and we assume that the hydraulic downstream flow line is representative of the downwind flow line. Glacier flow lines are calculated with the

Table 3. Off-Glacier Meteorological Stations and Seasonal Lapse Rates

Glacier	Melt Season Lapse Rate Off Glacier (°C/km)	Station	Location (Latitude, Longitude)	Elevation (m asl)	Distance to Glacier (km)
Haut Glacier d'Arolla	−5.8	Col du Grand-Saint-Bernard[a]	45.87 7.17	2472	30.3
		Sion	46.22 7.33	482	33.4
		Château d'Oex	46.48 7.14	1029	66.1
		Evolène	46.11 7.51	1825	16.7
Place	−5.2	Place Ridge[a]	50.43 −122.62	2075	2.3
		Pemberton	50.3 −122.74	204.3	15
Juncal Norte	−5.2	Portillo[a]	−32.83 −70.12	3000	24.3
		Aconcagua en Chacabuquito	−32.85 −70.51	1030	44.1
		Vilcuya	−32.86 −70.47	1100	40.5

[a]Stations used as a base for the extrapolation to x_0.

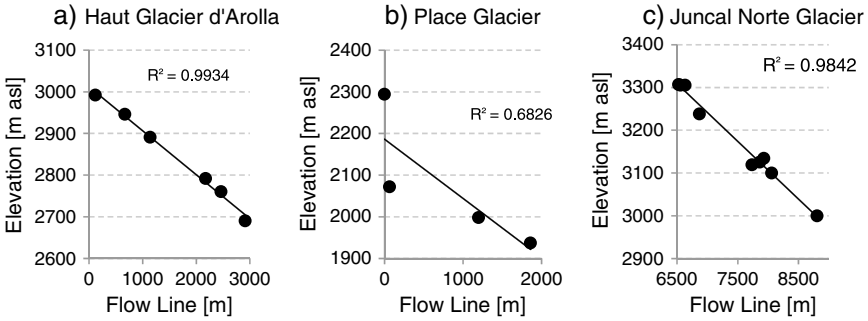

Figure 2. Elevation of air temperature stations (indicated in Figure 1) versus their distance along flow line. A linear relation is fitted. The distance along the flow line is measured in each glacier from the estimated origin point of katabatic winds (x_0).

TopoToolbox in MATLAB [*Schwanghart and Kuhn*, 2010] (Figure 1). Following the coordinate system defined by *Greuell and Böhm* [1998], calculated flow lines are projected over the horizontal plane and flow lines values were assigned based on the meteorological station locations. As the hydraulic flow line calculated for Place Glacier using TopoToolbox presented spatial discontinuities, we used the hydrological processing tools in SAGA GIS software package (http://www.saga-gis.org) for the Place Glacier calculations [*Shea and Moore*, 2010]. In Figure 2, we show the relation between elevation and distance along the flow line for meteorological stations on each glacier. An approximate linear relation indicating a constant slope between stations is observed on Haut Glacier d'Arolla and Juncal Norte Glacier. However, at Place Glacier, AWS1 is not aligned with the rest of the stations and the constant slope assumption is only fulfilled from AWS2.

In order to define an air temperature that is representative of off-glacier conditions, we extrapolate off-glacier hourly mean air temperatures from the nearest or highest elevation external station to the approximate center of the upper part or accumulation area of each glacier using seasonal mean lapse rates. These off-glacier lapse rates are calculated for each region using the available stations for the area (Table 3). The center of the accumulation area, hereinafter referred to as x_0, is selected by visual inspection and represents the origin in space of the katabatic wind or the theoretical point where the air parcel enters the layer influenced by the glacier [*Greuell and Böhm*, 1998; *Petersen et al.*, 2013]. *Greuell and Böhm* [1998] argue that x_0 depends on the geometry of each glacier and, as long as the nature of its dependence is not clear, it remains an empirical variable. Theoretically, x_0 is the point where the climatic sensitivity to off-glacier temperature variations is equal to one. Below this point the cooling effect of the glacier wind should be observed and the climate sensitivity will be reduced. An important requirement for choosing the x_0 parameter is to allow a sufficient distance for the development of density-driven winds. Following the notation of *Greuell and Böhm* [1998], the extrapolated temperature and elevation at x_0 are referred to as T_0 and z_0, respectively.

In Figure 3 we present average values and standard deviations of air temperature measured over the glacier surface for T_0 percentiles of 0–10th, 45–55th, and 90–100th. At Haut Glacier d'Arolla, air temperature follows a positive linear relation with the flow line and elevation for low values of T_0 (percentile 0–10th, $T_0 < -2.6$°C), which is consistent with negative temperature lapse rates and an indication that katabatic development is limited. On the other hand, when T_0 values are high (percentile 90–100th, $T_0 > 8.5$°C), air temperatures along the flow line decrease for $x < 1500$ m, which is consistent with katabatic wind effects [*Greuell and Böhm*, 1998]. Over the glacier tongue, air temperatures increase along the flow line, which suggests a higher climatic sensitivity to external air temperature changes. *Anslow et al.* [2008] found a similar air temperature distribution at South Cascade Glacier, Washington, USA, and noted the presence of an air temperature minimum at glacier midlevels.

Place Glacier exhibits a similar air temperature decrease along the flow line when off-glacier temperatures are high (percentile 90–100th, $T_0 > 11.4$°C). However, negative lapse rates are not observed over the lower section of Place Glacier. At Juncal Norte Glacier, where measurements are made only on the lower portion of the glacier ($z < 3300$ m asl and $x > 6500$ m), the air temperature decrease that is characteristic of katabatic effects is not evident. Instead, we observe that lapse rates become more negative (from -5 to -12°C/km) at higher values of T_0.

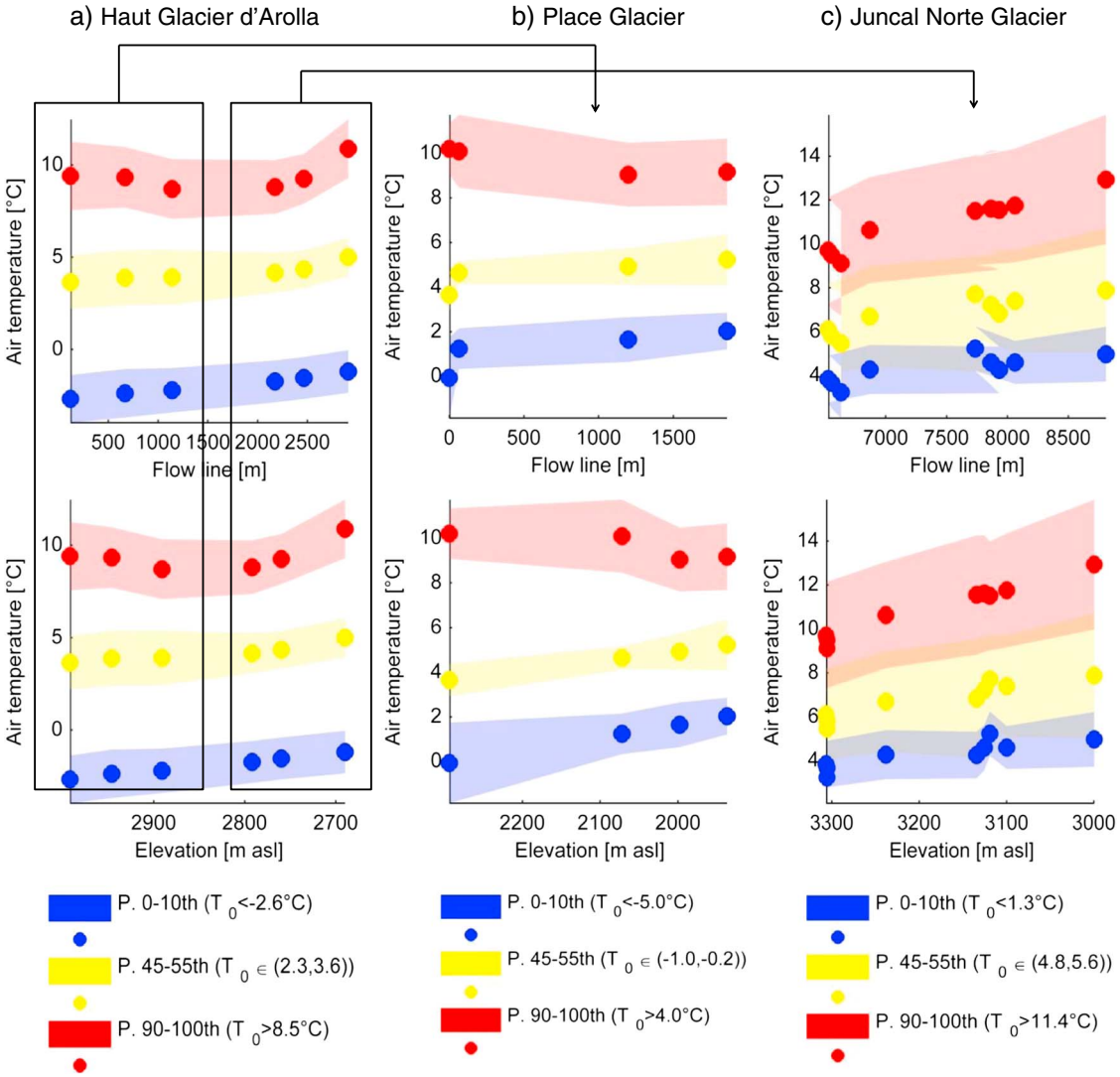

Figure 3. Air temperature recorded at T-loggers along the flow line and classified according to three percentile ranges of the T_0 variable defined in the original GB model. Top (bottom) row shows variation of air temperature with respect to the distance along the flow line (elevation). Dots represent the average temperature at the respective T-logger for time steps of T_0 values within selected percentiles. Colored bounds correspond to standard deviations. Reference values for each T_0 percentile range are added in parenthesis. We add two reference frames to conceptually relate air temperature data from the upper and lower sections of Haut Glacier d'Arolla to data in Place and Juncal Norte Glaciers, respectively.

Based on the results above, we calculate lapse rates at Place and Juncal Norte Glaciers with all observations (Figure 4). At Haut Glacier d'Arolla we distinguish between the three upper (ud) and the three lower stations (ld). At Place Glacier and in the upper section of Haut Glacier d'Arolla, lapse rates change from negative to positive values for increasing off-glacier temperatures. Conversely, lapse rates calculated at Juncal Norte Glacier and on the lower section of Haut Glacier d'Arolla remain negative with increasing off-glacier temperatures, but their magnitude also increases. At Juncal Norte Glacier, the increase in the lapse rate magnitude corresponds to a better correlation between air temperature and elevation (Figure 4). In contrast, at Place Glacier and in the upper part of Haut Glacier d'Arolla, an increase in off-glacier temperatures is followed by a reduction in correlation coefficients, which suggests that elevation is not a good predictor of air temperature under katabatic wind conditions. Under warm external conditions, air temperature is well-correlated with elevation over the glacier tongue, but not in the upper part of the glacier, where the correlation coefficient is weak. Additionally, we notice that the abrupt change in lapse rates of Place Glacier appears at the same temperature ($T_0 = 6–7°C$) found by *Shea and Moore* [2010] as the onset of katabatic wind development.

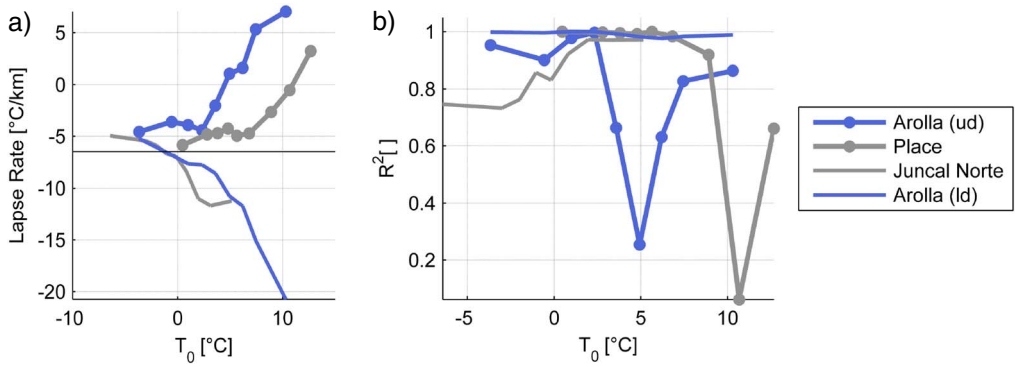

Figure 4. (a) Variation of average lapse rates and (b) respective correlation coefficients of air temperature and elevation as a function of off-glacier air temperatures (represented using T_0 percentiles). The environmental lapse rate (−6.49°C/km) is added as reference in Figure 4a. Lapse rates at Haut Glacier d'Arolla are calculated for the three upper T-loggers (upper data, ud) and the three lower T-loggers (lower data, ld).

To complement this exploratory analysis, we investigate the relations between air temperature distribution and wind effects. Wind distribution plots at the AWS within the glacier basins during the field experiment (see location in Figure 1) are based on the same classification of T_0 percentiles (Figure 5). Haut Glacier d'Arolla shows an up-valley wind (northerly) within the percentiles 0–10th of T_0 (<-2.6°C) (Figure 5a). When T_0 values are higher, the northerly wind component is not observed and the wind direction is dominated by down-glacier (southerly) winds (Figures 5b and 5c). AWS 4 at Place Glacier shows consistent down-glacier (easterly) winds within the entire T_0 range (Figures 5a–5c), though the greatest frequency occurs at higher values of T_0 (>11.4°C) (Figure 5c). Juncal Norte Glacier shows consistent down-glacier (southerly) winds within the entire T_0 range (Figures 5a–5c), with the exception of up-valley winds for percentiles 90–100th of T_0 (>4.0°C) (Figure 5c). According to *Petersen and Pellicciotti* [2011], these warm up-valley winds erode katabatic winds during the afternoon. They also observed that katabatic winds generated in the upper part of the glacier result in weak correlations between air temperature and elevation, while strong correlations are observed when katabatic winds are absent.

Two main conclusions from this exploratory data analysis section form the basis for our following analyses. First, when T_0 values are low, negative lapse rates close to the standard environmental lapse rate are sufficient to describe air temperature measurements over the entire glacier elevation range. Second, when T_0 values are high, air temperature decreases down-glacier within the upper part of the flow line, before increasing over the glacier tongue.

4. Modeling

4.1. A Modified Version of the Greuell and Böhm Model

The GB model solves the energy balance of an air parcel traveling down along an infinite glacier slope at a temperature of 0°C (Figure 6) [*Greuell and Böhm*, 1998]. The energy balance equation is

$$H\frac{\mathrm{d}\theta}{\mathrm{d}t} = -C_H(T - T_s)u \tag{1}$$

where H (m) is the height of the glacier wind layer, θ (°C) is the potential temperature, C_H ( ) is the bulk transfer coefficient for heat, T (°C) is the air temperature, T_S (°C) is the surface temperature, and u (m/s) is the glacier wind speed along the glacier surface [*Greuell and Böhm*, 1998].

The down-glacier wind speed u is assumed constant. If we consider the adiabatic variation of temperature due to changes in elevation along the glacier surface, we obtain

$$T = \theta + \Gamma_d \tan(\alpha)x \tag{2}$$

where Γ_d (°C/m) is the dry adiabatic lapse rate, α (°) is the mean glacier slope, and x (m) the distance along the flow line or flow path length.

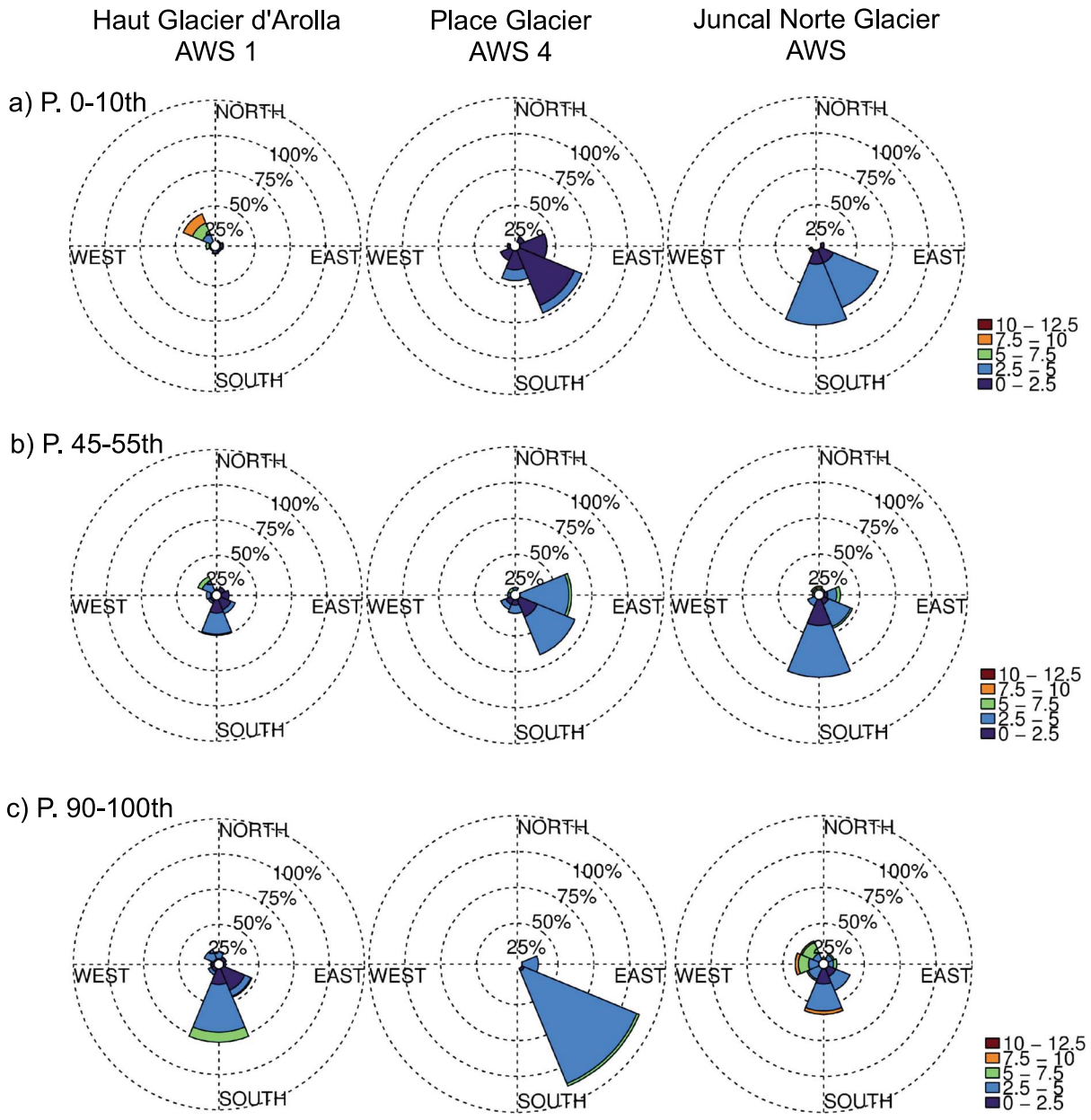

Figure 5. Wind roses at three representative AWS in respective glaciers. Wind distribution is shown for three percentiles ranges of the T_0 values. Wind speed in the legend is shown in m/s.

Greuell and Böhm [1998] considered that $T_s = 0$°C and that the term H/C_H is constant along the flow path length. In that way, solving the differential equation on x, the resulting equations of the energy balance are the following (see *Greuell and Böhm* [1998] for details in the derivation):

$$T(x) = (T_0 - T_{eq})\exp\left(-\frac{x - x_0}{L}\right) + T_{eq} \quad (3)$$

$$L = \frac{H\cos(\alpha)}{C_H} \quad (4)$$

$$T_{eq} = bL \quad (5)$$

$$b = \Gamma_d \tan(\alpha) \quad (6)$$

where $T(x)$ (°C) is the air temperature over the glacier as a function of the flow path length, T_0 (°C) is the air temperature at x_0, T_{eq} (°C) is the air temperature at $x = \infty$, L (m) is the characteristic length, x_0 (m) is the location

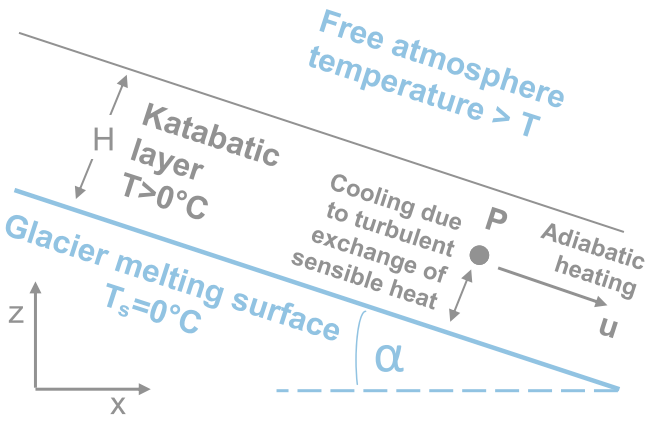

Figure 6. Schematic representation of the original GB model. The large dot P represents the air parcel considered in the model (adapted from *Greuell and Böhm* [1998] with permission of the authors and the International Glaciological Society).

were the air parcel enters the katabatic layer influenced by the glacier, b (°C /m) is a modified dry adiabatic lapse rate, and α (°) is the mean glacier slope. In contrast to *Greuell and Böhm* [1998], we use the symbol L and not L_R for the characteristic length, in order to avoid confusion with lapse rates (later referred to as LR).

The GB model is able to describe air temperature distributions during katabatic events. However, by definition, the model cannot describe the observed air temperature increase over glacier tongues as it assumes a glacier slope with an infinite length and no boundary conditions for large x values. Under these assumptions, air temperature converges to T_{eq} as x tends to infinity. However, our exploratory analyses suggest that during warm conditions, models of near-surface air temperature over melting glacier termini lack an important advected or entrained heat source. We thus introduce a new term that attempts to reproduce the observed behavior of air temperature over the entire extent of the studied glaciers. We will call this model a modified version of the original GB model, or ModGB model. The new term consists of an empirical factor (K(°C)) that multiplies the distance along the flow line ($x - x_0$), which is normalized using the length scale of the original GB model (L) and accounts for the observation that temperatures become warmer down valley. The factor K can be interpreted as the temperature increase from x_0 to L_R due to nonadiabatic processes, i.e., the influence of additional heat sources.

$$T(x) = (T_0 - T_{eq})\exp\left(-\frac{x - x_0}{L}\right) + T_{eq} + \underbrace{K\left(\frac{x - x_0}{L}\right)}_{\text{NEW TERM}} \quad (7)$$

4.2. Model Evaluation

In order to evaluate the ability of the ModGB model to describe the observed patterns of air temperature described in section 3.2, we fit the model to the observations using the katabatic layer height (H) and the new term (K) as tuning parameters. At each study site, we test the model under different scenarios of data availability and we use the calibrated model to extrapolate air temperatures over the entire glacier extent. Model is then evaluated using the root-mean-squared error (RMSE) of estimated temperatures. The model is fit to air temperature data that are averaged within T_0 intervals of 1°C. Given the results of the section 3.2, we adjust the modified GB model (keeping $K \neq 0$) only when T_0 is above 0°C and both katabatic cooling and glacier tongue warming effects are observed, i.e., at Haut Glacier d'Arolla and Juncal Norte Glacier. We compare the resulting RMSE of the ModGB model to the ones obtained from the original GB model and lapse rates. We note here that the original GB model is only calibrated for glaciers sections where the katabatic effect on air temperature was observed and T_0 is above 0°C (i.e., Place Glacier and the upper section of Haut Glacier d'Arolla).

Table 4. Topographic Parameters for the ModGB and GB Models

Parameter	Haut Glacier d'Arolla	Place	Juncal Norte
x_0 (m)	542	970	7998
z_0 (m asl)	3075	2294	5154
x_f (m)	5156	3077	16467
z_f (m asl)	2567	1841	2901
α (°)	6.28	12.14	14.90

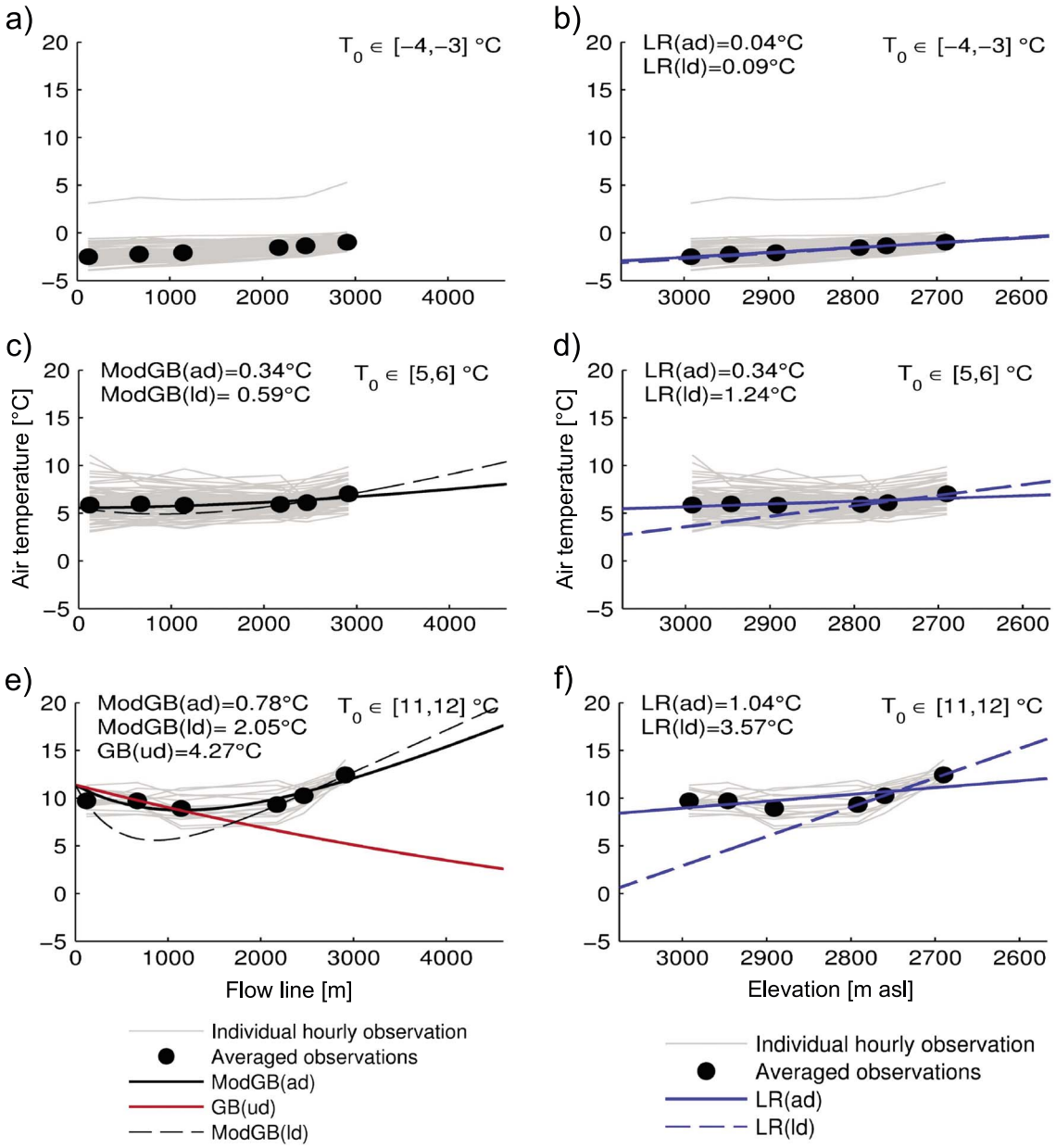

Figure 7. Examples of model fitting for Haut Glacier d'Arolla. We show the average observed data within T_0 ranges for each location (black dots), individual hourly observations (grey lines), and results of the ModGB model (black lines), the GB model (red lines), and lapse rates (blue lines). Air temperatures are shown as a function of the distance along the (a, c, and e) flow line relative to x_0 and (b, d, and f) elevation. Models were fitted to data along different glacier sections (upper data (ud), lower data (ld), and all data (ad)) and the RMSE (for each model) is calculated for the entire glacier.

In contrast to the original application of the GB model, we use the katabatic layer height (H) as a calibration parameter instead of the length-scale term (L). A similar approach by *Petersen et al.* [2013] is justified by our focus on the air temperature distribution and not on the climatic sensitivity of on-glacier conditions to external changes [e.g., *Greuell and Böhm* [1998]]. The katabatic layer height also provides a more direct physical interpretation than the length-scale parameter.

In order to obtain physically meaningful values of the selected parameters selected for calibration, the GB and ModGB model calibrations were consider successful when the katabatic layer height (H) converged to values lower than 100 m. As a reference, *Greuell and Böhm* [1998] calculated a value of $H = 17$ m for Pasterze Glacier.

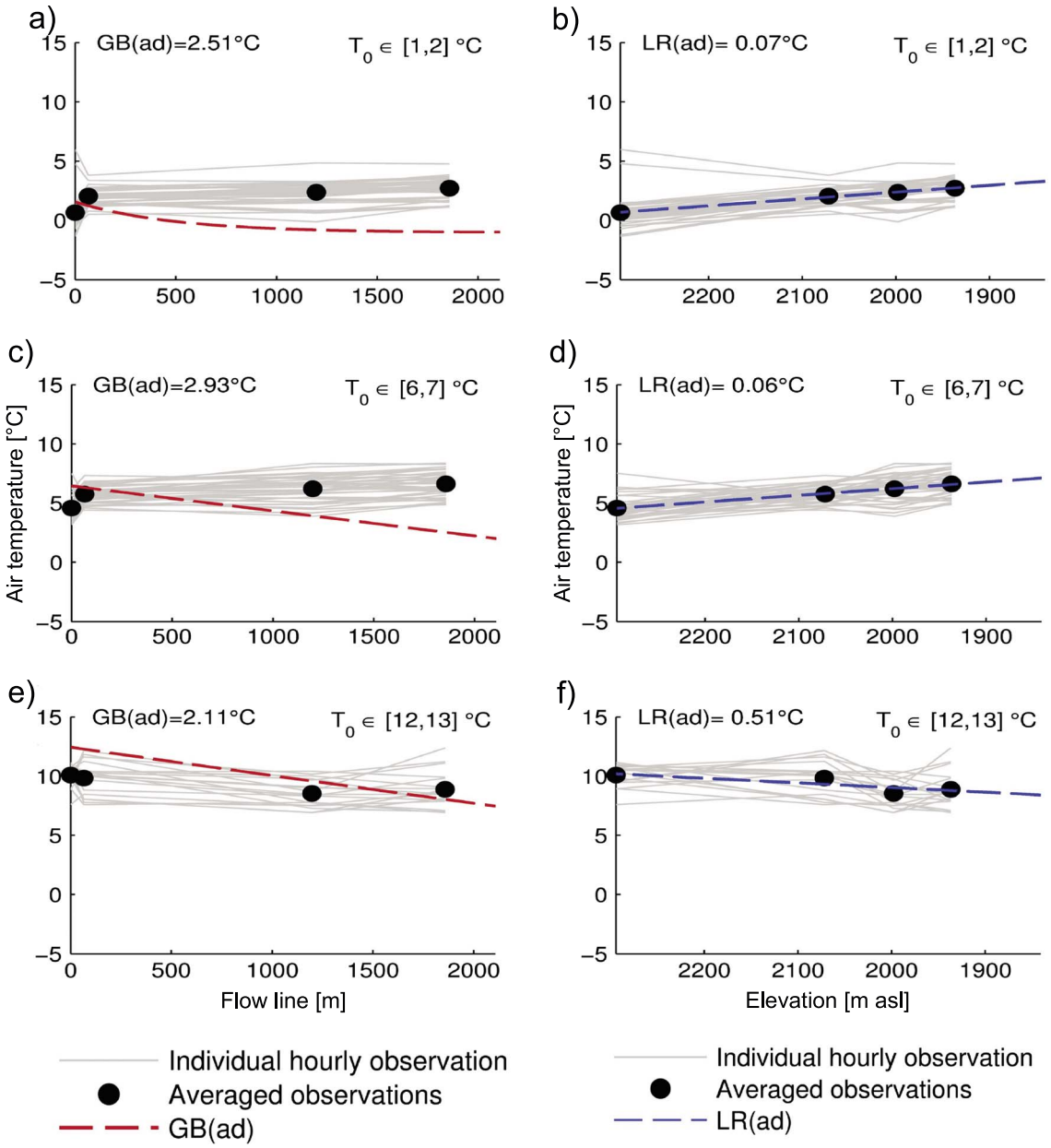

Figure 8. Examples of model fitting for Place Glacier. We show the average observed data within T_0 ranges for each location (black dots), individual hourly observations (grey lines), and results of the GB model (red lines) and lapse rates (blue lines). Air temperatures are shown as a function of the distance along the (a, c, and e) flow line relative to x_0 and (b, d, and f) elevation. Models were fitted to data of the entire glacier (all data, ad). The RMSE is shown for each model.

Topographic parameters used to fit the GB and ModGB models are given in Table 4. The mean glacier slope is estimated using the katabatic wind origin (x_0) and the values x_f and z_f, which correspond to the distance along the flow line and the elevation of the final point of the glacier, respectively.

5. Results

Binned air temperature distributions along the three study glaciers and the fitted models are shown in Figures 7–9. At Haut Glacier d'Arolla (Figure 7) we fit the original GB model, the ModGB model and the lapse rates to the data collected along the entire glacier and compare their performances. Additionally, we fit the ModGB model and lapse rates using only the three lowest T-loggers (lower data, ld) and evaluate their ability to estimate air temperatures recorded at the three upper T-loggers (upper data, ud). Finally, we fit the original GB model

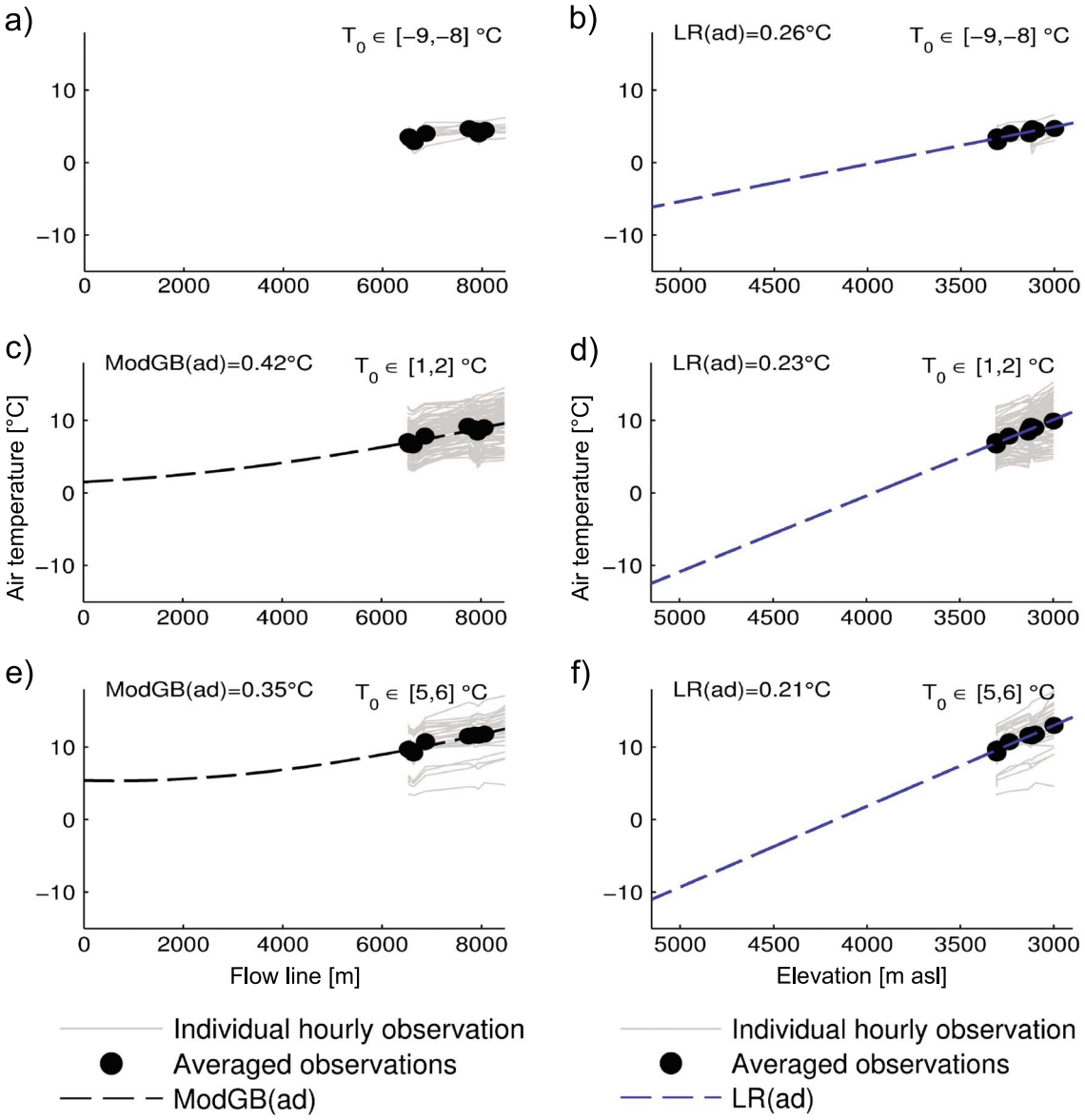

Figure 9. Examples of model fitting for Juncal Norte Glacier. We show the average observed data within T_0 ranges for each location (black dots), individual hourly observations (grey lines), and results of the ModGB model (black lines) and lapse rates (blue lines). Air temperatures are shown as a function of the distance along the (a, c, and e) flow line relative to x_0 and (b, d, and f) elevation (right column). Models were fitted to data along the lower glacier section (lower data, ld) and extrapolated to the upper area for comparison purposes. The RMSE is shown for each model.

using only the upper data and evaluate its performance to estimate air temperatures recorded over the glacier tongue. The ModGB model gives the best temperature estimates at Haut Glacier d'Arolla when values of T_0 are greater than 5°C (Figures 7a, 7c, and 7e). While the standard lapse rate approach correctly reproduces air temperature distribution for cold off-glacier conditions, its performance clearly decreases for higher temperatures (Figures 7b, 7d, and 7f). The original GB model correctly describes the behavior of the upper glacier data, but it fails to describe the warming over the glacier tongue (Figure 7e). With increased ambient temperatures, the ModGB (ad) model performance is superior to that of lapse rates (ad) in describing air temperature distribution along the entire glacier. Extrapolation of temperatures with the ModGB (ld) provides reduced errors along the entire glacier length when compared to lapse rates (ld) and the original GB model (ud) (Figures 7e and 7f). Nevertheless, RMSE values for the ModGB (ad) model also increase with T_0 (Figures 7c and 7e).

At Place Glacier (Figure 8), we attempt to fit the original GB model, but results are poor (Figures 8a, 8c, and 8e). As the data from the lower part of the glacier do not indicate significant additional warming inputs, we

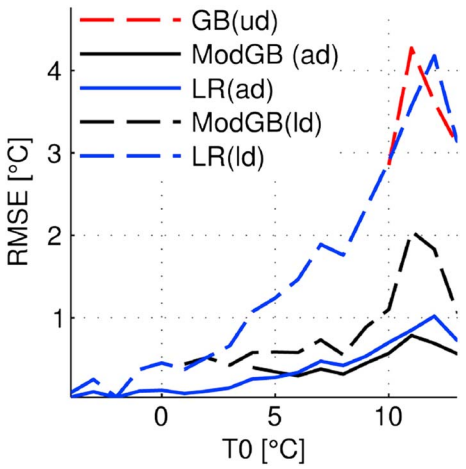

Figure 10. Comparison of the RMSE of adjusted models as a function of T_0 values for Haut Glacier d'Arolla.

do not fit a modified GB model. In the next section, we suggest and discuss the possible reasons for this result. On the other hand, lapse rates are able to reproduce the observed air temperature distribution, but the obtained RMSE values increase with T_0 (Figures 8b, 8d, and 8f).

At Juncal Norte Glacier (Figure 9), lapse rates perform better than the ModGB model in simulating air temperature measurements for all T_0 ranges. Notably, we observe large differences (>15°C) in the extrapolated air temperatures at high-elevation sites, where no data are available for model validation (Figures 9e and 9f).

In Figure 10, we compare RMSE values resulting from the model fitting at Haut Glacier d'Arolla for all T_0 bins. For T_0 values higher than 6°C, the ModGB (ad) model shows the lowest RMSE values, which are up to 32% lower than the ones obtained from LR (ad). Additionally, when only measurements from the lower glacier section are used for model calibration, the ModGB (ld) model gives the lowest errors for warm conditions (> 3°C). In this case, the ModGB (ld) model yields up to 68% lower RMSE values than the ones obtained from LR (ld). The original GB model, calibrated using only measurements

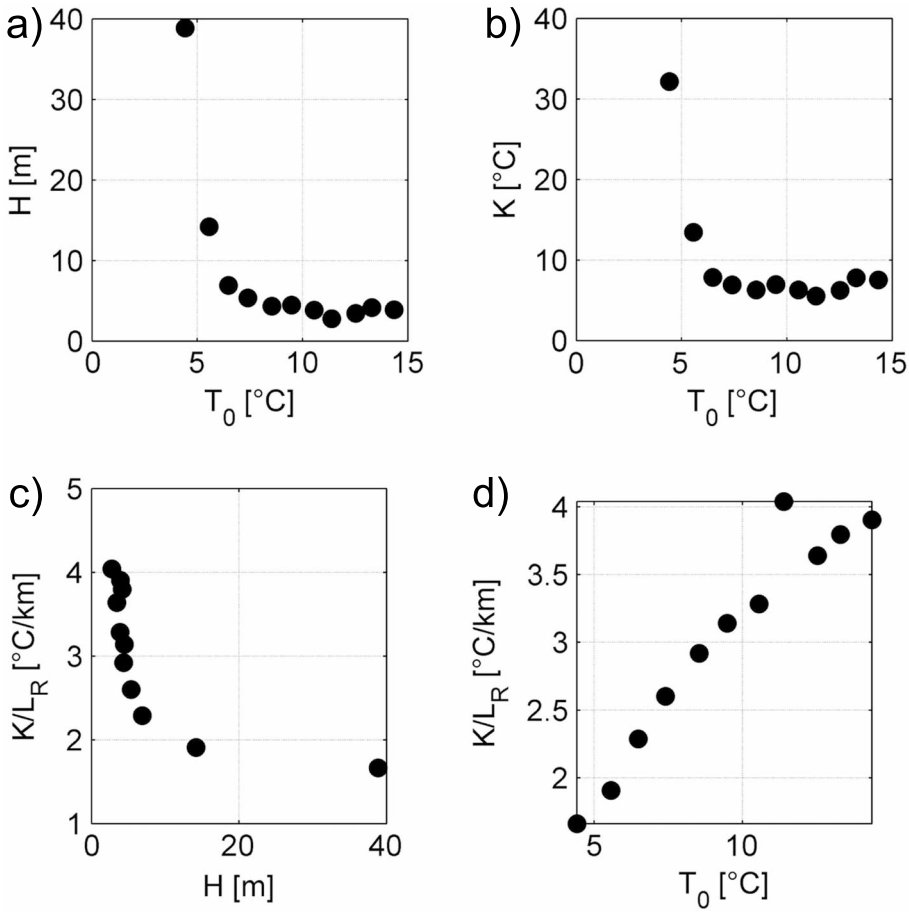

Figure 11. Relations between fitted parameters of the ModGB model and T_0 values for Haut Glacier d'Arolla. H is the katabatic layer thickness, K is the new term of the ModGB model, and K/L_R represents the magnitude of the temperature increase with the distance along the flow line.

of the upper part (GB (ud)), shows a similar performance to a lapse rate calibrated using data only from the glacier tongue.

In Figure 11 we show the relations between the tuned parameters values of the ModGB (ad) model for Haut Glacier d'Arolla. We show relations between the fitted parameters (H and K) and the T_0 bins. The katabatic layer height (H) and the empirical parameter (K) decrease for T_0 values above 4°C and converge to values of 5 m and 7°C, respectively (Figures 11a and 11b). In Figure 11c, we compare the adjusted katabatic layer height to the slope of the linear relation between air temperature and the distance along the flow line (K/L_R). This quantity represents the magnitude of the temperature increase with the distance along the flow line. K/L_R rapidly increases for low values of H, and increases with T_0 (Figure 11d). For T_0 values of approximately 10°C, the rate of air temperature increase along the glacier flow line (K/L_R) reaches 4°C per horizontal kilometer.

6. Discussion

Our results indicate that on-glacier lapse rates should only be used to describe air temperature distributions when ambient temperatures are low. In the absence of substantial temperature differences between the surrounding air mass and the glacier surface, katabatic flows are not generated and lapse rates have similar magnitudes to the commonly used environmental lapse rate (−6.49°C/km) (Figure 4). In contrast, high off-glacier temperatures drive the glacier surface to the melting point and create a constant boundary condition at 0°C allowing the development of katabatic winds [*Oerlemans*, 1998; *Oerlemans and Grisogono*, 2002]. These down-glacier winds transport cold air to lower elevations, which decrease the air temperature differences between the upper and lower sections of the glacier. This effect reduces the magnitude of the negative lapse rates and even results in positive lapse rates in some cases. We propose that additional heat sources will also affect the temperature of the descending air parcel. This results in steeply negative lapse rates at the lower sections of large valley glaciers (Figure 4).

While the investigated literature suggests that synoptic winds, entrainment from upper warm layers, turbulent mixing with up-valley winds, and heat advection from valley walls disrupt the katabatic wind layer [*van den Broeke*, 1997b; *Greuell and Böhm*, 1998; *Oerlemans and Grisogono*, 2002; *Munro*, 2006; *Jiskoot and Mueller*, 2012], it is difficult to identify exactly which physical processes are responsible for this phenomenon in each glacier. Up-valley winds found by *Petersen and Pellicciotti* [2011] erode katabatic winds during the afternoon in Juncal Norte Glacier, but these are not clearly seen at Haut Glacier d'Arolla. In fact, katabatic winds are strengthened in this glacier during the warmest hours of the day. Cross-glacier variability at Juncal Norte Glacier only showed small differences probably related to shading effects. In the case of Place Glacier, *Munro and Marosz-Wantuch* [2009] suggested that the shape of the upper glacier area favors the entrainment of synoptic winds, which could explain the poor fit of the original GB model to observed data. While it is clear that longwave radiation emitted from the valley walls increases melt rates on glacier surfaces [*Ohmura*, 2001; *Hock*, 2003; *Anslow et al*., 2008; *Jiskoot and Mueller*, 2012], it is not evident that is able to affect fast-moving air masses.

Our results show that under warm conditions, a modified Greuell and Böhm model is the best option to describe the observed air temperature distribution over Haut Glacier d'Arolla, in comparison to the original GB model and linear lapse rates. Furthermore, when data from the upper portions of Haut Glacier d'Arolla are not used for model tuning and models are evaluated along the entire glacier extent, the ModGB model produces considerably better results than the ones obtained by lapse rates. This suggests an improved ability to extrapolate air temperatures based on measurements from the glacier tongue (Figure 7). Applying this result to the Juncal Norte Glacier data, we suggest that air temperatures at high-elevation sites may be considerably warmer than those predicted by lapse rates derived from low-elevation on-glacier observations. In fact, for warm external conditions the tongue lapse rates are steeper than for low T_0 values and produce very low temperatures at high-elevation sites (<-10°C, Figure 9). Our results support those obtained by *Petersen and Pellicciotti* [2011], who demonstrated that steep negative lapse rates at the tongue of Juncal Norte Glacier are associated with warm conditions and strong correlation coefficients between air temperature and elevation, which might be used to justify the use of these lapse rates in extrapolating to high-elevation sites [*Ragettli et al*., 2013]. Nevertheless, the presence of katabatic winds, results in weakly negative or even positive lapse rates over upper glacier sites.

Our results for Haut Glacier d'Arolla further suggest that using the original GB model for distributing air temperature along the glacier will lead to a strong underestimation of air temperature on the glacier tongue. This is a direct consequence of the fact that the original model only considers the katabatic effect and adiabatic heating and does not account for external sources of heating. An alternative solution is the use of spatially variable values for the katabatic boundary layer height, as suggested by *Petersen et al*. [2013]. Indeed, the katabatic layer height is certainly affected and modified along the glacier flow line by the entrainment of warm air masses from aloft [*van den Broeke*, 1997a, 1997b; *Oerlemans*, 2010]. The GB model, however, assumes a spatially uniform H. To justify the use of a spatially variable H, *Petersen et al*. [2013] argue that the model should be used in a piecewise application of different H values, i.e., different model configurations are used for each location. We decided not to include this approach in our comparison exercise, because, in contrast to *Petersen et al*. [2013], all the models used in this article keep the same values for their parameters along the entire glacier extent. However, we note that the final results of *Petersen et al*. [2013] show an increasing katabatic layer height with the glacier flow line, which is consistent with the mixing of the katabatic layer with the warm surrounding atmosphere.

An interesting result of this study was the failure of the original GB model when applied to Place Glacier. This is likely due to the fact that two assumptions of the GB model are not fulfilled for this glacier. First, the meteorological stations on Place Glacier are not located along a linear profile with a constant slope (see Figure 2b). Second, this glacier is also exposed from both southerly and northerly directions, which can modify the thermal regime of the glacier surface due to the entrainment of external air masses. Thus, the glacier shape, and in particular the existence of a well-defined glacier termini that allows for funneling and convergence, is a requirement for the application of models that distribute air temperature based on the glacier flow line. In glaciers without a well-defined tongue, local winds may be weaker and the entrainment of synoptic winds and heat advection more relevant. Specific measurements directed to capture those processes would be useful in the case of cirques or plateau-type glaciers, e.g., T-loggers close to valley walls and meteorological stations on very exposed sites. Due to the convergent flow lines, an interesting case to analyze would be multiple-basins feeding into one tongue. In fact, *Munro* [2006] found colder air temperatures at the convergence points of the katabatic flow field than on the tongue of Peyto Glacier, Canadian Rockies.

As the models were fitted to observed air temperatures binned in 1°C intervals, the observed variability (grey lines in Figures 7–9) may be a result of different weather conditions at each location and different amounts and type of cloudiness in particular. At all sites, cloudy conditions were mainly associated with cold temperatures and negative lapse rates along the entire glacier extent, so the results of the ModGB model should not be largely affected. In the case of Juncal Norte Glacier, more than 90% of the observations were collected under clear-sky conditions, which are typical during the summer season in the dry Andes of central Chile [*Pellicciotti et al*., 2008; *Ragettli and Pellicciotti*, 2012].

From the analysis of the calibrated parameters, H and K appear to converge to constant values, which likely reflect the full development of a katabatic layer in a sufficiently warm atmosphere. Additional temperature data that cover the full extent of the glacier would be useful in order to study the transferability of these parameters and detail their variation as a function of external temperatures. These parameters are empirical in nature, because they depend on individual properties of each glacier. The rest of the parameters used in the model can also be dependent on additional features of the glacier environment that were not analyzed in this study. In particular, x_0 may vary depending on the elevation of the snowline which might affect fetch length, and T_0 may be affected by the variability of off-glacier lapse rates. Further studies should focus on the specific sensitivity analysis of the model to these parameters.

7. Conclusions

In this paper, we have analyzed three data sets of 2 m air temperature measurements collected over glaciers at different latitudes and with different characteristics, with the aim to understand the observed spatial variability in air temperature and identify the most appropriate approach for data extrapolation. Air temperature is a key input to glacier mass balance and glacier hydrological models, which are used for projections of future runoff from glacierized catchments. Previous studies have demonstrated that temperature lapse rates are one of the parameters to which glaciohydrological models are most sensitive [e.g., *Ragettli and Pellicciotti*, 2012;

Pellicciotti et al., 2014]. Observations and models of temperature gradients over melting snow and ice surfaces are thus critical for the generation of accurate melt estimates.

In practice, temperatures are often extrapolated using spatially uniform linear lapse rates. An alternative model proposed by *Greuell and Böhm* [1998] describes the effect of katabatic boundary layer formation on temperatures over melting glaciers. In this model, air temperatures are calculated from the equilibrium of adiabatic heating with cooling due to the sensible heat exchange with the glacier surface. Analyses of the three detailed data sets, however, suggest that other mechanisms might play a role over melting glaciers, especially for warm conditions under which melt occurs. We therefore suggest a modification of the GB model, built by including an additional term that accounts for the heating of an air parcel traveling down valley along well-confined glacier tongues, which provide a dominant longitude direction and a strong funneling effect.

We summarize our main findings as follows:

1. This study has demonstrated that air temperature follows similar spatial patterns on three glaciers of considerably different geographical, topographical, and climatic features. At all three sites, during off-glacier conditions below 0°C, air temperature follows negative lapse rates, which are close in magnitude to the environmental lapse rate (−6.49°C/km). In contrast, observations from the upper regions of melting glaciers show that positive off-glacier temperatures generate katabatic effects that result in positive lapse rates over the upper glacier section. At the same time, these warm conditions produce strong negative lapse rates over well-defined glacier termini. The combination of these two effects generates a spatial minimum of air temperature over the middle section of the glacier. The temperature increase with distance along the flow line over the glacier tongue may be caused by different processes induced by the warm atmosphere and increased shortwave radiation in the case of clear-sky days. These processes may include the entrainment of warm air from upper layers, mixing with up-valley winds and heat convection generated by enhanced terrain irradiance.
2. To characterize the observed temperature patterns, a linear term that captures the increase in temperature due to heat advection and/or entrainment was added to the GB thermodynamical wind model. The modified model was calibrated using available observations and its performance compared to that of the original model and linear lapse rates.
3. During cold off-glacier conditions (<0°C), negative linear lapse rates that are similar to the environmental lapse rate are sufficient to describe the observed air temperature distributions. For warm off-glacier conditions (when melt occurs), the modified GB model for air temperature estimation provides a clear improvement over both the original GB model and linear lapse rates. To apply the ModGB using only off-glacier data, it would be beneficial to better understand how model parameters vary as a function of external temperatures.
4. During warm off-glacier conditions (>0°C), the extrapolated method used can result in large differences in the estimation of high-elevation air temperatures. At Juncal Norte Glacier, where only data collected on the glacier tongue are available, air temperatures at high elevation estimated by the ModGB model can be more than 15°C higher than those estimated with lapse rates. This would result in large differences in estimates of glacier ablation and have thus a strong impact on glacier mass balance and runoff simulations.

Our results highlight the importance of distributed field measurements over melting glaciers and can be used to improve energy and mass balance simulations of glacierized catchments. Further research should incorporate additional temperature data sets in order to characterize the onset of katabatic wind conditions, the location of the minimum air temperature over mountain glaciers and quantify the variation of the parameters of the ModGB model as a function of external air temperatures. Measurements directed to identify specific processes like heat convection from valley walls and shading effects could be also useful. Additionally, direct measurements of sensible and latent heat fluxes along the glacier flow line and profiles of the near-surface katabatic layer will allow further model refinements and improve process-based models of glacier melt in the context of a changing climate.

Acknowledgments

We thank the Editor and three anonymous reviewers for their useful comments on the paper, which helped improve it. The authors would like to thank all the people involved in the data collection in Switzerland, Canada and Chile. Collection of meteorological data at Place Glacier was funded through the Western Canadian Cryospheric Network (WC2N), as part of the Canadian Foundation for Climate and Atmospheric Science (CFCAS). Lidar data from Place Glacier were collected as part of a C-CLEAR effort to develop Lidar environmental applications, and we gratefully acknowledge the contributions of M. Demuth, C. Hopkinson, and B. Menounos. Alvaro Ayala acknowledges the Becas Chile scholarship program (Comisión Nacional de Investigación Científica y Tecnológica de Chile, CONICYT) and Paolo Burlando for support at ETH. The authors also thank W. Greuell for his valuable comments. The data shown in this paper can be available pending an e-mail request to ayala@ifu.baug.ethz.ch.

References

Anslow, F. S., S. Hostetler, W. R. Bidlake, and P. U. Clark (2008), Distributed energy balance modeling of South Cascade Glacier, Washington and assessment of model uncertainty, *J. Geophys. Res.*, *113*, F02019, doi:10.1029/2007JF000850.

Arnold, N., I. Willis, and M. Sharp (1996), A distributed surface energy-balance model for a small valley glacier. I. Development and testing for Haut Glacier d'Arolla, Valais, Switzerland, *J. Glaciol.*, *42*(140), 77–89.

Aster GDEM Validation Team (2011), ASTER Global Digital Elevation Model version 2.
Bown, F., A. Rivera, and C. Acuña (2008), Recent glacier variations at the Aconcagua basin, central Chilean Andes, *Ann. Glaciol.*, *48*, 43–48, doi:10.3189/172756408784700572.
Brock, B., I. Willis, M. J. Sharp, and N. S. Arnold (2000), Modelling seasonal and spatial variations in the surface energy balance of Haut Glacier d'Arolla, Switzerland, *Ann. Glaciol.*, *31*(1996), 53–62.
Carturan, L., F. Cazorzi, F. De Blasi, and G. D. Fontana (2014), Air temperature variability over three glaciers in the Ortles-Cevedale (Italian Alps): Effects of glacier disintegration, intercomparison of calculation methods, and impacts on mass balance modeling, *Cryosphere Discuss.*, *8*, 6147–6192, doi:10.5194/tcd-8-6147-2014.
Corripio, J., and R. Purves (2005), Surface energy balance of high altitude glaciers in the central Andes: The effect of snow penitentes, in *Climate and Hydrology in Mountain Areas*, edited by C. De Jong, D. Collins, and R. Ranzi, pp. 15–27, John Wiley, Hoboken, N. J.
Dadic, R., J. Corripio, and P. Burlando (2008), Mass-balance estimates for Haut Glacier d'Arolla, Switzerland, from 2000 to 2006 using DEMs and distributed mass-balance modeling, *Ann. Glaciol.*, *49*, 22–26, doi:10.3189/172756408787814816.
Denby, B., and W. Greuell (2000), The use of bulk and profile methods for determining surface heat fluxes in the presence of glacier winds, *J. Glaciol.*, *46*(154), 445–452, doi:10.3189/172756500781833124.
Gardner, A. S., and M. Sharp (2009), Sensitivity of net mass-balance estimates to near-surface temperature lapse rates when employing the degree-day method to estimate glacier melt, *Ann. Glaciol.*, *50*(50), 80–86, doi:10.3189/172756409787769663.
Gardner, A. S., M. J. Sharp, R. M. Koerner, C. Labine, S. Boon, S. J. Marshall, D. O. Burgess, and D. Lewis (2009), Near-surface temperature lapse rates over Arctic glaciers and their implications for temperature downscaling, *J. Clim.*, *22*(16), 4281–4298, doi:10.1175/2009JCLI2845.1.
Garreaud, R. D., M. Vuille, R. Compagnucci, and J. Marengo (2009), Present-day South American climate, *Palaeogeogr. Palaeoclimatol. Palaeoecol.*, *281*, 180–195, doi:10.1016/j.palaeo.2007.10.032.
Greuell, J., M. van den Broeke, W. Knap, C. Reijmer, P. Smeets, and I. Struijk (1994), PASTEX: A glacio-meteorological experiment on the Pasterze (Austria), Utrecht.
Greuell, W., and R. Böhm (1998), 2 m temperatures along melting mid-latitude glaciers, and implications for the sensitivity of the mass balance to variations in temperature, *J. Glaciol.*, *44*(146), 9–20.
Hannah, D. M., A. M. Gurnell, and G. R. Mcgregor (2000), Spatio-temporal variation in microclimate, the surface energy balance and ablation over a cirque glacier, *Int. J. Climatol.*, *20*(7), 733–758, doi:10.1002/1097-0088(20000615)20:7<733::AID-JOC490>3.0.CO;2-F.
Hock, R. (1999), A distributed temperature-index ice-and snowmelt model including potential direct solar radiation, *J. Glaciol.*, *45*(149), 101–111.
Hock, R. (2003), Temperature index melt modelling in mountain areas, *J. Hydrol.*, *282*(1–4), 104–115, doi:10.1016/S0022-1694(03)00257-9.
Hock, R. (2005), Glacier melt: A review of processes and their modelling, *Prog. Phys. Geogr.*, *29*(3), 362–391, doi:10.1191/0309133305pp453ra.
Hock, R., and B. Holmgren (2005), A distributed surface energy-balance model for complex topography and its application to Storglaciaren, Sweden, *J. Glaciol.*, *51*(172), 25–36.
Hoinkes, H. (1954), Beiträge zur Kenntnis des Gletscherwindes, *Arch. Meteorol. Geophys. Bioklimatol.*, *B6*, 36–53.
Jiskoot, H., and M. S. Mueller (2012), Glacier fragmentation effects on surface energy balance and runoff: Field measurements and distributed modelling, *Hydrol. Process.*, *26*(12), 1861–1875, doi:10.1002/hyp.9288.
Klok, E., and J. Oerlemans (2002), Model study of the spatial distribution of the energy and mass balance of Morteratschgletscher, Switzerland, *J. Glaciol.*, *48*(163), 505–518, doi:10.3189/172756502781831133.
Michlmayr, G., M. Lehning, G. Koboltschnig, H. Holzmann, M. Zappa, R. Mott, and W. Schöner (2008), Application of the Alpine 3D model for glacier mass balance and glacier runoff studies at Goldbergkees, Austria, *Hydrol. Process.*, *3949*(July), 3941–3949, doi:10.1002/hyp.
Moore, R. D., and M. N. Demuth (2001), Mass balance and streamflow variability at Place Glacier, Canada, in relation to recent climate fluctuations, *Hydrol. Process.*, *15*(18), 3473–3486, doi:10.1002/hyp.1030.
Munro, D. S. (2006), Linking the weather to glacier hydrology and mass balance at Peyto glacier, in *Peyto Glacier*: *One Century of Science*, pp. 135–178, National Hydrology Research Institute Science Report #8.
Munro, D. S., and M. Marosz-Wantuch (2009), Modeling ablation on Place Glacier, British Columbia, from Glacier and off-glacier data sets, *Arct. Antarct. Alp. Res.*, *41*(2), 246–256, doi:10.1657/1938-4246-41.2.246.
Oerlemans, J. (1998), The atmospheric boundary layer over melting glaciers, *Clear Cloudy Bound. Layers*, *R. Netherlands Acad. Arts Sci.*
Oerlemans, J. (2010), *The Microclimate of Valley Glaciers*, Igitur, Utrecht Publishing & Archiving Services, Universiteitsbibliotheek Utrecht, Utrecht.
Oerlemans, J., and B. Grisogono (2002), Glacier winds and parameterisation of the related surface heat fluxes, *Tellus, Ser. A*, 440–452.
Ohmura, A. (2001), Physical basis for the temperature-based melt-index method, *J. Appl. Meteorol.*, *40*(4), 753–761, doi:10.1175/1520-0450(2001)040<0753:PBFTTB>2.0.CO;2.
Pellicciotti, F., B. Brock, U. Strasser, P. Burlando, M. Funk, and J. Corripio (2005), An enhanced temperature-index glacier melt model including the shortwave radiation balance: Development and testing for Haut Glacier d'Arolla, Switzerland, *J. Glaciol.*, *51*(175), 573–587, doi:10.3189/172756505781829124.
Pellicciotti, F., J. Helbing, A. Rivera, V. Favier, J. Corripio, J. Araos, J. E. Sicart, and M. Carenzo (2008), A study of the energy balance and melt regime on Juncal Norte Glacier, semi-arid Andes of central Chile, using melt models of different complexity, *Hydrol. Process.*, *22*, 3980–3997, doi:10.1002/hyp.7085.
Pellicciotti, F., S. Ragettli, M. Carenzo, and J. McPhee (2014), Changes of glaciers in the Andes of Chile and priorities for future work, *Sci. Total Environ.*, *493C*, 1197–1210, doi:10.1016/j.scitotenv.2013.10.055.
Petersen, L., and F. Pellicciotti (2011), Spatial and temporal variability of air temperature on a melting glacier: Atmospheric controls, extrapolation methods and their effect on melt modeling, Juncal Norte Glacier, Chile, *J. Geophys. Res.*, *116*, D23109, doi:10.1029/2011JD015842.
Petersen, L., F. Pellicciotti, I. Juszak, M. Carenzo, and B. Brock (2013), Suitability of a constant air temperature lapse rate over an Alpine glacier: Testing the Greuell and Böhm model as an alternative, *Ann. Glaciol.*, *54*(63), 120–130, doi:10.3189/2013AoG63A477.
Pigeon, K., and H. Jiskoot (2008), Meteorological controls on snowpack formation and dynamics in the southern Canadian Rocky Mountains, *Arct. Antarct. Alp. Res.*, *40*(4), 716–730, doi:10.1657/1523-0430(07-054).
Ragettli, S., and F. Pellicciotti (2012), Calibration of a physically based, spatially distributed hydrological model in a glacierized basin: On the use of knowledge from glaciometeorological processes to constrain model parameters, *Water Resour. Res.*, *48*, W03509, doi:10.1029/2011WR010559.
Ragettli, S., G. Cortés, J. McPhee, and F. Pellicciotti (2013), An evaluation of approaches for modelling hydrological processes in high-elevation, glacierized Andean watersheds, *Hydrol. Process.*, doi:10.1002/hyp.10055.
Reid, T. D., M. Carenzo, F. Pellicciotti, and B. W. Brock (2012), Including debris cover effects in a distributed model of glacier ablation, *J. Geophys. Res.*, *117*, D18105, doi:10.1029/2012JD017795.
Schwanghart, W., and N. J. Kuhn (2010), TopoToolbox: A set of MATLAB functions for topographic analysis, *Environ. Modell. Softw.*, *25*(6), 770–781, doi:10.1016/j.envsoft.2009.12.002.

Shea, J., S. Marshall, and J. Livingston (2004), Glacier distributions and climate in the Canadian Rockies, *Arct. Antarct. Alp. Res.*, *36*(2), 272–279.
Shea, J. M., and R. D. Moore (2010), Prediction of spatially distributed regional-scale fields of air temperature and vapor pressure over mountain glaciers, *J. Geophys. Res.*, *115*, D23107, doi:10.1029/2010JD014351.
Shea, J. M., R. D. Moore, and K. Stahl (2009), Derivation of melt factors from glacier mass-balance records in western Canada, *J. Glaciol.*, *55*(189), 123–130, doi:10.3189/002214309788608886.
Strasser, U., J. Corripio, F. Pellicciotti, P. Burlando, B. Brock, and M. Funk (2004), Spatial and temporal variability of meteorological variables at Haut Glacier d'Arolla (Switzerland) during the ablation season 2001: Measurements and simulations, *J. Geophys. Res.*, *109*, D03103, doi:10.1029/2003JD003973.
Tachikawa, T., M. Hato, M. Kaku, and A. Iwasaki (2011), Characteristics of ASTER GDEM version 2, *Geosci. Remote Sens. Symp.*, 3657–3660.
van den Broeke, M. R. (1997a), Momentum, heat, and moisture budgets of the katabatic wind layer over a midlatitude glacier in summer, *J. Appl. Meteorol.*, *36*(1981), 763–774.
van den Broeke, M. R. (1997b), Structure and diurnal variation of the atmospheric boundary layer over a mid-latitude glacier in summer, *Boundary Layer Meteorol.*, *83*, 183–205.
Vihma, T., E. Tuovinen, and H. Savijärvi (2011), Interaction of katabatic winds and near-surface temperatures in the Antarctic, *J. Geophys. Res.*, *116*, D21119, doi:10.1029/2010JD014917.